JACS
JOURNAL OF THE AMERICAN CHEMICAL SOCIETY
Article
pubs.acs.org/JACS

Complex Surface Diffusion Mechanisms of Cobalt Phthalocyanine Molecules on Ag(100)

Grażyna Antczak,*[,‡] Wojciech Kamiński,[‡] Agata Sabik,[‡] Christopher Zaum,[†] and Karina Morgenstern[§]

[‡]Institute of Experimental Physics, University of Wrocław, Wrocław, Poland
[†]Leibniz University Hannover, Hannover, Germany
[§]Chair for Physical Chemistry I, Ruhr-Universität Bochum, Bochum, Germany

Supporting Information

ABSTRACT: We used time-lapsed scanning tunneling microscopy between 43 and 50 K and density functional theory (DFT) to explore the basic surface diffusion steps of cobalt phthalocyanine (CoPc) molecules on the Ag(100) surface. We show that the CoPc molecules translate and rotate on the surface in the same temperature range. Both processes are associated with similar activation energies; however, the translation is more frequently observed. Our DFT calculations provide the activation energies for the translation of the CoPc molecule between the nearest hollow sites and the rotation at both the hollow and the bridge sites. The activation energies are only consistent with the experimental findings, if the surface diffusion mechanism involves a combined translational and rotational molecular motion. Additionally, two channels of motion are identified: the first provides only a channel for translation, while the second provides a channel for both the translation and the rotation. The existence of the two channels explains a higher rate for the translation determined in experiment.

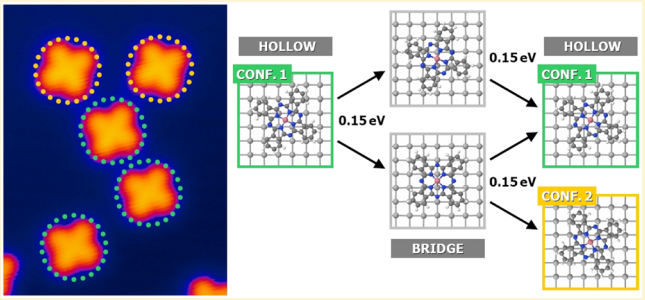

I. INTRODUCTION

Phthalocyanine (Pc) molecules provide quite an increase in complexity compared to frequently studied small inorganic molecules, the complex of 57 (58 for H_2Pc) interconnected atoms of different identity (for CoPc: 1 cobalt, 8 nitrogen, 32 carbon, and 16 hydrogen atoms), interacting with a number of surface atoms. The investigation of the surface motion of large organic molecules is in its nascent form despite the fact that understanding the motion of complex organic molecules is an important task. Organic molecules are frequently utilized as building blocks in organic nanodevices and electronics.[1,2] In this respect the Pc are model molecules that are, among others, investigated with reference to optoelectronics,[3] sensors,[4] and quantum computing.[5] Among this class, the CoPc and its diffusion are of particular importance as the magnetic moment of the central Co atom makes this molecule attractive for spin and magnetic applications. In fact, its magnetic moment and Kondo effect were widely investigated.[6−8]

Surface diffusion is central to many technological processes, such as crystal growth, catalysis, sintering, etc. It influences the stability of functional, technologically important materials. The motion of adatoms on surfaces was widely investigated, and the basic mechanism of motion is quite well understood, although not completely unveiled.[9] However, it is still quite a challenge to probe the motion of slightly bigger objects, such as dimers and trimers on the surface[10−12] or small molecules such as water[13] and CO.[14] The coupling of CO bending modes with translational lateral motion on Ni(111) was demonstrated by Dobbs and Doren[15] using molecular dynamics simulations. The surface diffusion of larger objects can be quite complicated. Recently, the motion of a single polymer molecule in the liquid/solid environment was shown to be desorption mediated.[16] The gold nanoclusters consisting of 140 Au atoms exhibit the collective slip-diffusion motion on the graphite, which involves the correlation of rotational motion of nanoclusters with lateral translation.[17] The interesting properties of Pc's have triggered a number of scanning tunneling microscopy (STM) studies of the quasi-isolated molecule at 5 K[18−20] and the molecule immobilized within the molecular layer at room temperature or above and imaged at 5 K.[18,21,22] What has hardly been tackled is the influence of temperature on the adsorption and motion of the molecules.

A few studies on other organic molecules revealed higher complexity in surface diffusion. The first direct investigation of a large organic molecule was conducted for the one-dimensional (1D) motion of 4-*trans*-2-(pyrid-4-yl-vinyl)benzoic acid (PVBA) on the anisotropic Pd(110) surface by Weckesser et al.[23] This study showed that the motion of this organic molecule can be described by the Arrhenius relation. The same group investigated the motion of C_{60} molecule on the same surface and showed the importance of a local reconstruction on the molecular mobility.[24] The activation energy for surface diffusion of a C_{60} molecule on the isolated surface was

Received: August 6, 2015
Published: November 19, 2015

DOI: 10.1021/jacs.5b08001
J. Am. Chem. Soc. 2015, 137, 14920−14929

determined by Loske et al.[25] with atomic force microscopy indirectly utilizing the islands nucleation theory. Schunack et al.[26] investigated in detail the motion of decacyclene (DC) and hexa-*tert*-butyldecacyclene (HtBDC) molecules on the Cu(110) surface. In their study they detected the presence of long jumps involved in the motion of molecules additionally to single jumps. Kwon et al.[27] probed the 1D motion of 9,10-dithioanthracene (DTA) molecule on the Cu(111) surface. They combined the STM and the density functional theory (DFT) study to show the active role of ligands for their motion. These ligands contain sulfur, which made the molecule stay on a 1D course. The same combined STM/DFT approach was used to show that anthraquinone (AQ) on Cu(111) can reversibly attach CO_2 molecules and plays the role of molecular carrier, changing the dimensionality of CO_2 motion.[28] The *n*-butane motion on Pt(111) and Cu(100) was studied using transition state theory by Raut and Fichthorn.[29] The conformational correlation in molecular hopping and directional anisotropy induced by a molecular degree of freedom was detected. Yokoyama et al. investigated the motion of tris(2-phenylpyridine)iridium(III) ($Ir(ppy)_3$) molecules on the Cu(111) surface.[30] They observed translational and rotational transitions of the molecule but characterized only the translational motion. The surface diffusion of molecules from the family of porphyrins, to which Pc belongs, started with the work of Eichberger et al.,[31] who investigated the motion of tetrapyridylporphyrin (TPyP) on Cu(111). They showed that the deformation of the molecule forces an almost 1D surface diffusion on this isotropic surface and observed translational motion with very sporadic rotational events, which allows the molecule to switch between energetically preferential directions. The motion of 2*H*-tetraphenylporphyrin (2HTPP) molecule was investigated by Bucher et al. on Cu(111).[32] Similarly to TPyP, the motion is almost 1D. The majority of the surface diffusion studies discussed so far utilized the STM to measure the map of adsorption sites visited by the investigated molecule. Ikanomov et al. utilized the STM to detect the diffusive noise during the motion of a CuPc and a 3,4,9,10-perylenetetracarboxylic dianhydride (PTCDA) on the Ag(100) surface.[33] From the noise they determined the effective characteristics of motion without gaining any insight into the mechanisms of the motion. For CuPc the authors determined an activation energy of 0.08 eV and a prefactor for diffusivity in the range of 10^{-8} cm^2/s.[33] An activation energy of 0.03 eV and a prefactor for diffusivity of 10^{-9} cm^2/s were reported in a refined analysis of the experimental data.[34] The unusually low activation energies and prefactors for diffusivity obtained in those studies are somehow surprising. The authors, however, did not take into account the unequal input of different atoms of the tip into the tunneling current during motion of large molecule. The noise fluctuation method can detect also the uncoupled rotational motion of molecules with rectangular shape as for example PTCDA.[35] Only two above studies combine the experimental work with DFT calculations of the diffusive paths in order to reveal the full complexity of the motion of the organic molecule, and thus the underlying reason for the observed behavior remains to be understood.

In this article we investigate the adsorption geometry of CoPc molecules and their motion on Ag(100). We performed measurements using a low-temperature scanning tunneling microscopy (LT-STM) and supported them with *ab initio* DFT calculations. This combination allows us to gain a detailed understanding of the complex motion. During the motion translation and rotation are correlated.

II. EXPERIMENTAL SECTION

The experiments were carried out in a low-temperature custom-built scanning tunneling microscope.[36] The Ag sample was cleaned by a combination of Ar^+ sputtering for 1 h (energy of 1.3 keV, sputtering current 3 μA) with annealing at 903 K for 6 min, followed by a combination of sputtering for 3 min (energy of 0.65 keV, sputtering current 2 μA) with annealing at 803 K for 1.5 min. The purity of the sample was checked by the STM, and the images were analyzed with WSxM.[37] Before evaporation the Knudsen cell was outgassed at 673 K for 3 days. CoPc molecules (Sigma-Aldrich) were deposited from a Knudsen cell kept at 752 K on the Ag(100) surface kept at 20 K. The sample with approximately 0.1 ML of CoPc molecules was transferred to the STM. The coverage of 1 ML corresponds to a sample that is covered by one layer of CoPc molecules adsorbed parallel to the surface. Both the purity of deposition and the coverage were checked by static measurement at 5 K. During the diffusion study the sample was kept at a fixed diffusion temperature ranging between 43 and 50 K. The temperature was controlled with a silicon diode (Lakeshore) and carefully stabilized over a few hours before every measurement to lower the influence of thermal drift. By determining the temperature drop between the position of the Si diode and the sample in a separate experiment and by using a calibration curve of the producers of the diode instead of the usually employed Chebychev polynoms, we are able to reduce the temperature uncertainty to below 0.25 K. The remaining thermal drift is eliminated from the data by tracking the position of a stable feature, usually the position of a step edge. We tracked the motion of 25−35 molecules over 2−11 h at 13 different temperatures. The investigation took in total 1683 images, from which 1437 were measured with a time interval between images of 195 s and 246 with a diffusion time interval of 390 s.

III. COMPUTATIONAL METHODOLOGY

The first-principles DFT calculations were performed with the Vienna simulation package (VASP, version 5.2).[38,39] The projector-augmented wave (PAW) method[39] was used with the gradient-corrected Perdew−Burke−Ernzerhof (PBE-GGA) exchange-correlation functional.[40] A plane-wave basis with a cutoff energy of 500 eV and **k**-points with the 4 × 4 × 1 Γ-centered Monkhorst−Pack mesh were used in all calculations. The convergence criteria for the relaxation process were changes in total energy lower than 10^{-4} eV and forces on the free atoms smaller than 0.03 eV/Å. The van der Waals (vdW) interactions were included using the scheme of Grimme[41] and appeared to be of crucial importance for proper determination of the adsorption energy. The use of PAW−PBE without vdW correction leads to the lack of energy minima for CoPc adsorption. We can reasonably assume that the energetic order of the translational to rotational barriers should hold for our system with more advanced vdW schemes[42,43] like PBE + vdW^{surf} or vdW-DF. A standard supercell approach was applied with the substrate represented by a slab of five Ag atomic layers, from which the three topmost layers were allowed to relax and the remaining two bottom Ag layers were fixed in their bulk positions. We used the equilibrium Ag bulk lattice constant of 4.15 Å, which is in good agreement with other theoretical investigations[44−46] and slightly bigger (≈1.5%) than the experimental value of 4.08 Å.[47] In our calculations we have used the 8 × 8 unit cell including 377 atoms in total: 320 of the Ag substrate and 57 of the CoPc molecule. Applying the 8 × 8 periodicity (see Figure 1a) is large enough to treat the CoPc molecule in its quasi-isolated state; however, this does not exclude possible intermolecular interaction effects, e.g.,

DOI: 10.1021/jacs.5b08001
J. Am. Chem. Soc. 2015, 137, 14920−14929

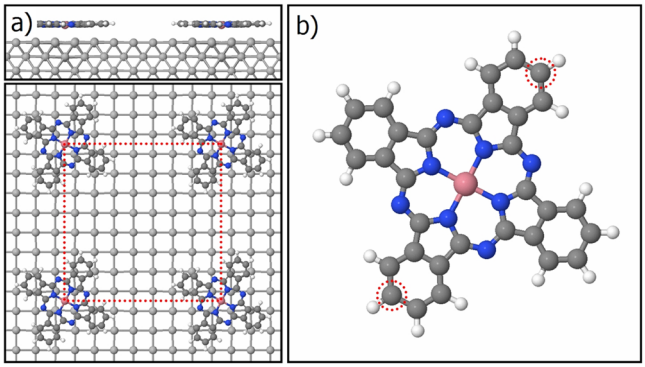

Figure 1. Arrangement of CoPc molecules in DFT calculations. (a) Side and top view of the CoPc molecule adsorbed on the Ag(100) surface. The 8 × 8 unit cell is marked by red dotted line. (b) Schematic of the CoPc molecule. The carbon atoms which x and y coordinates are frozen during the rotation are marked by red dotted circles. Color code for the atoms: silver (light gray), cobalt (pink), nitrogen (blue), carbon (gray), and hydrogen (white).

substrate-mediated electrostatic interactions. Note that the molecule-to-molecule distance in our 8 × 8 supercell is 23.5 Å, similar to the experimental mean molecule−molecule distance of 27.0 ± 0.7 Å. The calculated adsorption energy of the CoPc molecule at the hollow site and at an orientation of 27.5° amounts to 6.21 eV and the distance of the molecular plane from surface layer to 2.78 Å. The CoPc molecule is negatively charged by 0.82 electrons received from the Ag substrate as calculated using the Bader analysis.[48] The diffusion characteristics were investigated using the constrained static model, which enables us to explore the potential energy landscape. The activation energies for the translation/rotation of the CoPc molecule have been determined in a stepwise, quasi-static manner by moving/rotating the molecule over the Ag(100) surface. For the translation we moved the CoPc molecule in the x direction by small steps (1/40 of the hollow-to-hollow distance) over the surface, with x and y coordinates of the central Co atom of the molecule frozen to keep the molecule on the transition path, and recorded the changes in the total energy of the system. The molecule was free to rotate during the hollow-to-hollow translation steps. For the rotation, we rotated the CoPc molecule by a small steps of 2.5° above the hollow or the bridge site with frozen x and y coordinates of three atoms of the CoPc molecule (the central Co atom and the two extremes carbon atoms marked by red dotted circles in Figure 1b) to fix the position and the orientation of the molecule and recorded the changes of the total energy on the whole transition path. At each step of the translation/rotation procedure the free atoms in both the Ag slab and the CoPc molecule were allowed to relax to their ground-state configuration. The dynamics of both the molecule and the underlying lattice was neglected in these studies. We do not expect a significant temperature influence at 43−50 K on the potential energy landscape and on the effective diffusion barriers; however, *ab initio* MD simulations performed at measurement temperature could give insight into that question as well as reveal the atomistic mechanism of the rotational and translational movements.

IV. RESULTS AND DISCUSSION

Geometry of Adsorption. After adsorption the molecules are randomly distributed on the surface (Figure 2) with a mean

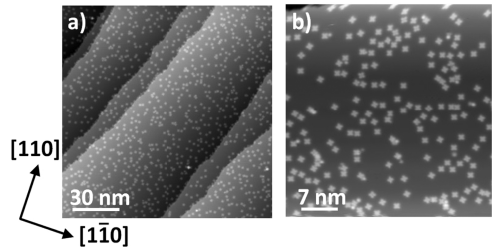

Figure 2. (a, b) Overview STM images of 0.1 ML of CoPc molecules deposited on Ag(100) surface at 5 K. Scanning conditions: (a) V = −397 mV, I = 28 pA, T = 5 K. (b) V = 289 mV, I = 51 pA, T = 5 K.

molecule−molecule distance of 27.0 ± 0.7 Å (308 distances measured between the centers of the molecules). A CoPc molecule is visible in the STM as a four-lobe protrusion, presented in Figure 3a; the same type of protrusion is observed

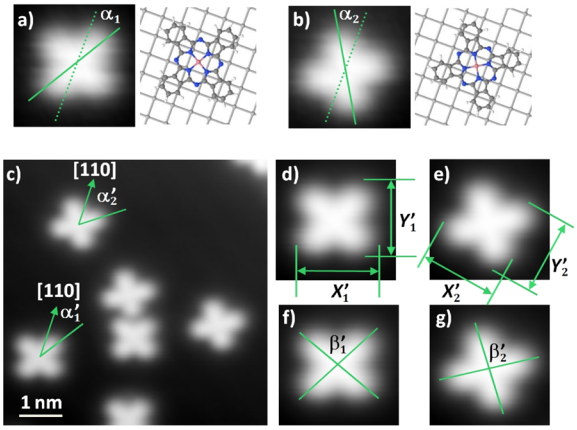

Figure 3. (a, b) Zoom into STM image of CoPc molecule imaged at 5 K together with schematics of CoPc molecule on Ag(100) surface in (a) configuration 1 and (b) configuration 2. Green lines mark orientation angle of molecule; dotted green line mark closed packed direction on the surface. (c−g) STM images of two configurations at 37 K. Indicated are in (c) orientation angles; (d, e) X' and Y' sizes of both configurations; and in (f, g) angles between molecular axes. Tunneling parameters: V = −397 mV, I = 28 pA, T = 5 K (a, b), and T = 37 K (c−g).

as for other Pc molecules.[18−20] The formation of dimers and trimers, shown in Figure S1 of the Supporting Information, is observed after extended annealing at 43−50 K. Larger clusters are not observed. We did not investigate the stability of objects larger than a monomer.

At 5 K, CoPc molecules are observed in two mirror-like equally probable configurations with a four-lobe shape, which resembles nicely the structural shape of the molecule (Figure 3a). Surprisingly, at around 37 K the image of a molecule looks rectangular with a ratio Y_1'/X_1' = 0.94 ± 0.03 for configuration 1 and Y_2'/X_2' = 0.87 ± 0.04 for configuration 2 (shown in Figure 3d,e). The mean value of angles between molecular axes, marked in Figure 3f,g (measured for 20 molecules), amounts to β_1' = 101.1 ± 0.9° for configuration 1 and β_2' = 96.9 ± 0.6° for configuration 2. The rectangular shape can be associated with the deformation of CoPc molecule on Ag(100). The deformation cannot be an STM artifact since both configurations have similar rectangular shape despite their different alignments with respect to the fast scanning direction. The deformation of the molecule by a shift of the central Co atom

DOI: 10.1021/jacs.5b08001
J. Am. Chem. Soc. 2015, 137, 14920−14929

out of planarity of the molecule was previously seen for adsorption on Si(100) at 437 K[49] and on Cu(111)[19,50] at 29 K. It is, however, not clear whether our deformation is also associated with the out-of-plane deformation of the molecule. Unfortunately, our calculations performed at 0 K are unable to reproduce the observed shape changes which are thermally induced.

Our calculations show that the most stable configuration of the molecule is with its central metal atom above the hollow site. The molecules are adsorbed in two equally probable, mirror-like configurations, shown in Figure 3a,b, together with the schematics of the orientation of the CoPc molecule with respect to the surface. The procedure of measuring the orientation angle is illustrated in Figure 3a–c. The molecule is rotated clockwise (+) or counterclockwise (−) with respect to the [110] direction. At 5 K, experimentally, the orientation angle is $\alpha_1 = +28.9 \pm 0.4°$ in configuration 1, while in configuration 2 is $\alpha_2 = -29.9 \pm 0.4°$ (see Figure 3a,b). Our theoretically determined orientation angle amounts to $\alpha_1 = +27.5°$ for configuration 1 and $\alpha_2 = -27.5°$ for configuration 2. These values are in fair agreement with the experimental values as well as with the value reported previously for the same system.[19] The change in the shape of the molecule at elevated temperatures is accompanied by an increase in the orientation angles to $\alpha_1' = +32.2 \pm 0.4°$ for configuration 1 and $\alpha_2' = -35.7 \pm 0.4°$ for configuration 2.

Effective Motion of CoPc on Ag(100). We start with exploration of the displacement of the CoPc molecule over the surface, which provides us with the effective motion of the molecule without insight into the elemental steps which constitute the molecular transport. CoPc molecules are immobile on Ag(100) at 5 K. Increasing the temperature to a value between 43 and 50 K allows tracking the motion of molecules over Ag(100) on the time scale of minutes. A movie which shows the typical motion of CoPc molecule is provided in the Supporting Information. Snapshots of the movie are shown in Figure 4. The motion is 2D, and the deformation of the molecule visible in STM images does not influence the dimensionality of motion. The motion along the [110] and [1−10] directions proceeds with the same probability. Figure 5 shows the values averaged for both ⟨110⟩ directions.

First, we explore a possible influence of the scanning tip onto the motion of a molecule by performing measurements with short and long waiting intervals between the images. With short waiting intervals, the tip scans image after image. The acquisition time of one image is 189 s, and a new image is started every 195 s. When long waiting intervals are applied, the tip scans again one image in 189 s, but a new image is only started after 390 s. The interaction time of the tip with a molecule is thus halved. As all data fall on one line in the Arrhenius graph in Figure 5, there are no measurable tip–molecule interactions influencing the surface diffusion.

The map of places visited by three CoPc molecules at 43 K is presented in Figure S2. The molecules make discrete jumps along ⟨110⟩ directions. Additionally, from our theoretical study we learn that only the hollow sites provide the stable equilibrium places for the molecules. That allows us to correlate the molecular displacements with the Ag(100) lattice spacing and by careful inspection of map of adsorption places visited by molecule, for every single set of STM images, decide if the molecule is jumping or not. The procedure excludes possible artificial displacements associated with the uncertainty of the reading of the position of the molecule's center-of-mass

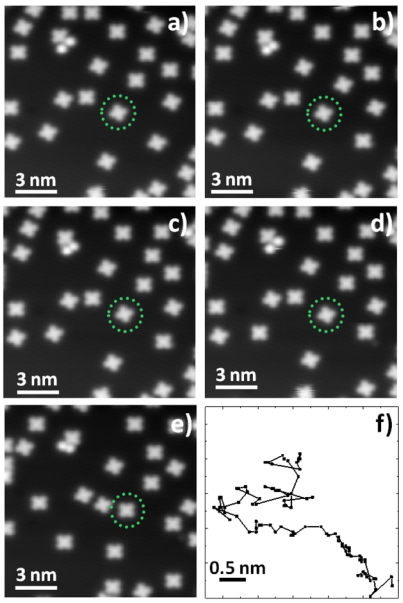

Figure 4. (a–e) STM images showing stages of surface diffusion of CoPc on Ag(100). Scanning conditions: $V = -397$ mV, $I = 28$ pA, $T = 49$ K. (f) The track of position of center-of-mass of the molecule (marked with green circles) during motion for 16 185 s at 49 K. The mean-square displacement of this molecule is 20 Å^2.

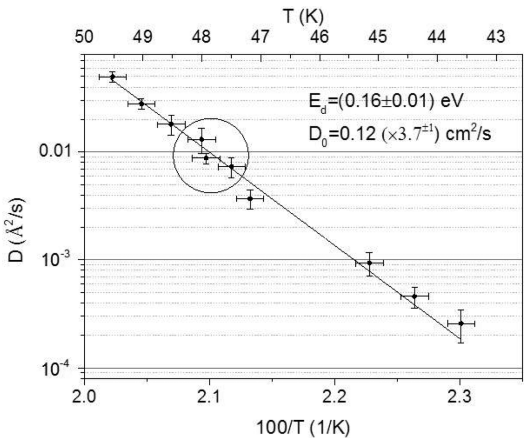

Figure 5. Arrhenius dependence of CoPc diffusivity in ⟨110⟩ directions. The scanning time of a frame is 189 s for all data. The circle marks the measurements with diffusion time interval of 390 s. For the rest of the data diffusion time interval of 195 s.

and the position of the reference feature used for thermal drift corrections from the Arrhenius plot. This is very important since at the lowest temperatures the molecule stays almost at one position for most images and drift induced displacements would add multiple times leading to an artificial mean-square displacement, which would cause an artificial bending of the Arrhenius plot at low temperatures.

Finally, we explore the energetics of the CoPc motion by probing the temperature dependence of the diffusivity D. The diffusivity is determined using the relation[9] $\langle \Delta x^2 \rangle = 2D\Delta t$, where $\langle \Delta x^2 \rangle$ is the mean-square displacement along [110] directions and Δt the diffusion time interval. The displacements of the center-of-mass were measured directly from series of STM images for at least 280 displacements per temperature, and consecutive displacements at the same temperature and time interval were accumulated. At 48 K we have 1560

DOI: 10.1021/jacs.5b08001
J. Am. Chem. Soc. 2015, 137, 14920–14929

displacements. The diffusion time interval is given by the time of the scanning of one STM image. From the Arrhenius plot of the diffusivity we determine the effective activation energy E_D for CoPc diffusion as 0.16 ± 0.01 eV and the prefactor for diffusivity D_0 as 0.03−0.44 cm^2/s.

Previous direct STM investigations performed for diffusion of organic molecules from the family of porphyrins were conducted at higher temperatures (above 280 K) and are associated with much higher activation energies of 0.71 for 2H-TPP[32] and 0.96 eV for TPyP.[31] The lower activation energy for CoPc can be associated with the planar form of the molecule. In both TPP and TPyP molecules the benzene rings of the molecule are attached to the central porphyrin macrocycle through a single bond, which allows higher flexibility and facilitates the saddle shape of those molecules.[31] Such a shape increases not only the activation energy but also causes the preferential motion in 1D.

The activation energy obtained in our study for the CoPc molecule is considerably larger than the values of 0.03 and 0.08 eV (in refs 34 and 33, respectively) determined for CuPc on Ag(100). However, these results were obtained by analyzing diffusive noise measured by STM. Our study shows that the CuPc molecule is immobile up to 60 K[51] so the analysis of diffusive noise greatly underestimates the value of the activation energy or other paths contribute to surface diffusion and the mechanism of motion of that molecule changes in the temperature range of 144−222 K, investigated in refs 33 and 34.

We obtain the prefactor of diffusivity in the range of 10^{-1} cm^2/s from the plot presented in Figure 5, higher than the standard value of 10^{-3} cm^2/s. Previously, a prefactor in the range 10^{-1} cm^2/s was associated with the presence of long jumps for the motion of DC and HtBDC molecules on the Cu(111) surface.[26] The presence of long jumps for the CoPc molecule might be responsible for the higher prefactor for diffusivity in our case as well. However, it also can be associated with the presence of several processes contributing to the surface diffusion. Unfortunately, it is not possible to extend the current study to higher temperatures to gain deeper insight into the problem, since the CoPc molecule at higher temperatures crosses under the tip multiple times creating diffusive noise and making the direct tracking of molecule position in the STM impossible.

Translational and Rotational Motion of CoPc Molecule. From the STM images obtained during the motion of CoPc molecules, shown in Figure 4, it is clear that the molecule translates and rotates during motion, with translation observed 4 times more frequently. During the motion, the molecule can be observed in a new adsorption site with or without a change of its configuration (rotation). In addition, the molecule can change its configuration without changing the adsorption site (see Figure 6a). To analyze these processes, we assume that if a transition occurs, then it happens only once per scanning cycle (no multiple jumps or rotations). This is possible because the measurements were made close to the onset temperature of motion.

As the STM provides us only with snapshots of diffusion stages without direct insight into diffusion paths or correlations of transitions, we envision three possible scenarios. The energetics emerging from all three scenarios are summarized in Table 1.

Scenario 1: All observed events are independent of each other. Then there are three types of elementary events present

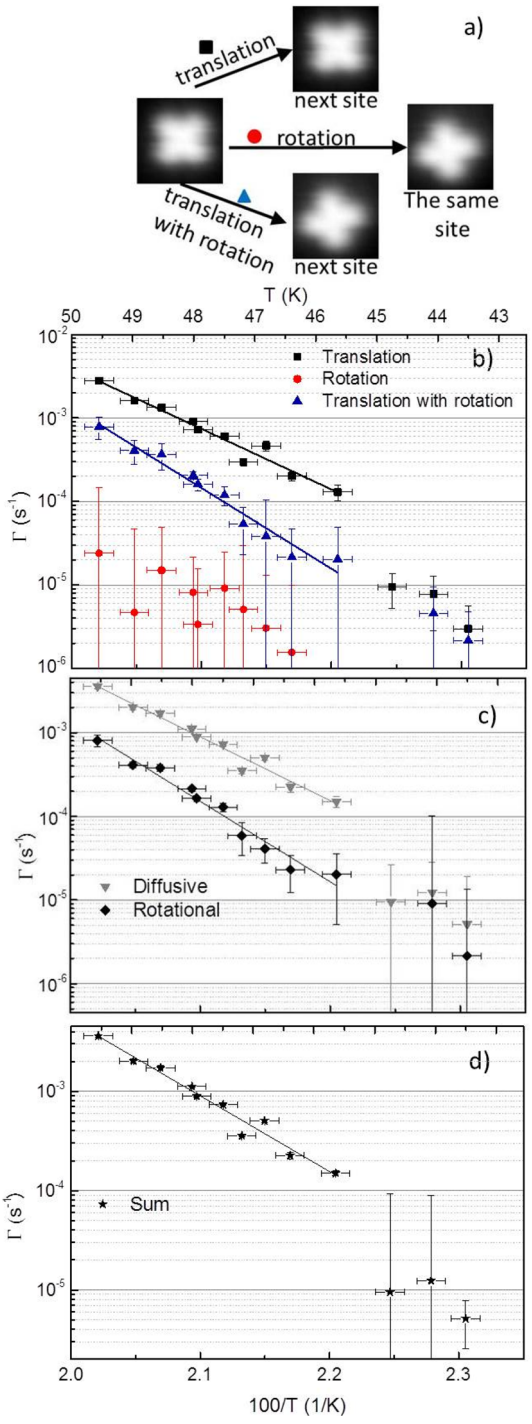

Figure 6. (a) STM images illustrating all observed transitions V = −397 mV, I = 28 pA, and T = 49 K. Plots of transitions rates: (b) rotations, translations, and translations with rotation, (c) diffusive and rotational, (d) sum.

on the surface: translation when a molecule is found in a new adsorption place in the same configuration, rotation when a molecule is observed at the same place but in a new configuration, and translation with rotation when a molecule is in a new place in a new configuration. The corresponding rates, shown in Figure 6b, provide us with energetics of two types transitions only. The small number of rotations (as visible in the error bars) does not allow fitting these data with confidence in contrast to translations and translations with

DOI: 10.1021/jacs.5b08001
J. Am. Chem. Soc. 2015, 137, 14920−14929

Table 1. Energetics of Possible Transitions Observed in Motion of CoPc on Ag(100)[a]

			E_D (eV)	D_0 (cm^2/s) or ν_0 (s^{-1})
experimental	effective		0.16 ± 0.01	0.12 ($\times 3.7^{\pm 1}$) cm^2/s
	scenario 1	translation	0.14 ± 0.01	1.28 ($\times 12.34^{\pm 1}$) × 10^{12} s^{-1}
		rotation with translation	0.18 ± 0.02	1.14 ($\times 6.93^{\pm 1}$) × 10^{15} s^{-1}
	scenario 2	diffusive	0.15 ± 0.01	9.18 ($\times 11.2^{\pm 1}$) × 10^{12} s^{-1}
		rotational	0.19 ± 0.01	2.39 ($\times 21.8^{\pm 1}$) × 10^{15} s^{-1}
	scenario 3	sum	0.15 ± 0.01	9.37 ($\times 11^{\pm 1}$) × 10^{12} s^{-1}
theory	rotation at hollow		0.28/0.31	
	translation at orientation of +27.5°		0.21	
	rotation at bridge		0.08/0.10	
	combined rotation with translation		0.15/0.15	

[a] E_D = activation energy for the process, D_0 = prefactor for diffusivity, and ν_0 = frequency prefactor.

rotation. Excluding the lowest points due to their statistic insufficiency, fitting the translation yields an activation energy of 0.14 ± 0.01 eV, and the frequency factor is between 1.04 × 10^{11} and 1.58 × 10^{13} s^{-1}. Rotation with translation can be fitted by an activation energy of 0.18 ± 0.02 eV and a higher than usual frequency factor between 1.65 × 10^{14} and 7.93 × 10^{15} s^{-1}.

Scenario 2: Only two independent events occur: a change in position (diffusive event) and a change in orientation (rotational event). In such a case translation with rotation is observed due to the occurrence of both events during the scan time. The Arrhenius plot illustrating such a scenario will separate diffusive and rotational events, and it is shown in Figure 6c. From the plot we determined the activation energies, for diffusive events, which require a change in the position of the molecule, the activation energy is 0.15 ± 0.01 eV, and the frequency prefactor is between 8.22 × 10^{11} and 1.02 × 10^{14} s^{-1}. There is an agreement between the activation energy for this event with the activation energy obtained from the temperature dependence of the diffusivity (Figure 5, effective in Table 1). This justifies the assumption of a lack of multiple jumps per scanning cycle and confirms that measurements were made close to the onset temperature. In the other plot we present the Arrhenius plot of all events which lead to a change in the configuration (rotational events). From the plot we determine the activation energy as 0.19 ± 0.01 eV and the frequency prefactor between 1.09 × 10^{15} and 5.22 × 10^{17} s^{-1} after excluding the three lowest points due to their statistical insignificance, visible in the large error bar associated with these measurements. We see that in this scenario the change in the configuration requires slightly higher activation energy than the change in the position of the molecule over the surface. Scenario 2 is providing very similar values to scenario 1. This happens because the diffusive events consist of translations from scenario 1 enlarged by translation with rotation, which shifts the plot upward and slightly increases its inclination. Whereas, rotational events are comparable to rotation with translation because a small number of rotations without a displacement of the center-of-mass is observed.

Scenario 3: All transitions are interconnected, and only one type of events is present. The separation of configuration change and translation happens in the transition state. Then we have to plot the sum of observed events, as shown in Figure 6d. This plot is different from the one of the dependence obtained from the temperature dependence of the diffusivity (Figure 5, effective in Table 1) because here the transitions with and without displacement of center-of-mass are taken into account. The plot gives us an activation energy of 0.15 ± 0.01 eV and frequency prefactors between 8.53 × 10^{11} and 1.03 × 10^{14} s^{-1}. This is in fair agreement with the standard attempt frequency prefactor in the range 10^{13} s^{-1}.[9]

Potential Energy Surface of CoPc−Ag(100) System. To explore which of the three scenarios is the valid one, we probe the potential energy surface for the CoPc on Ag(100) system using DFT calculations. First, we investigate the total energy of the system at various orientation angles with a CoPc molecule adsorbed with the central atom above the hollow site, as determined above. The top panel of Figure 7 shows the changes of the total energy of the system during rotation for orientation angles between −45° and +45°. The bottom panel illustrates the top views of the selected intermediate geometries (see A to F in Figure 7) from the rotational path of the

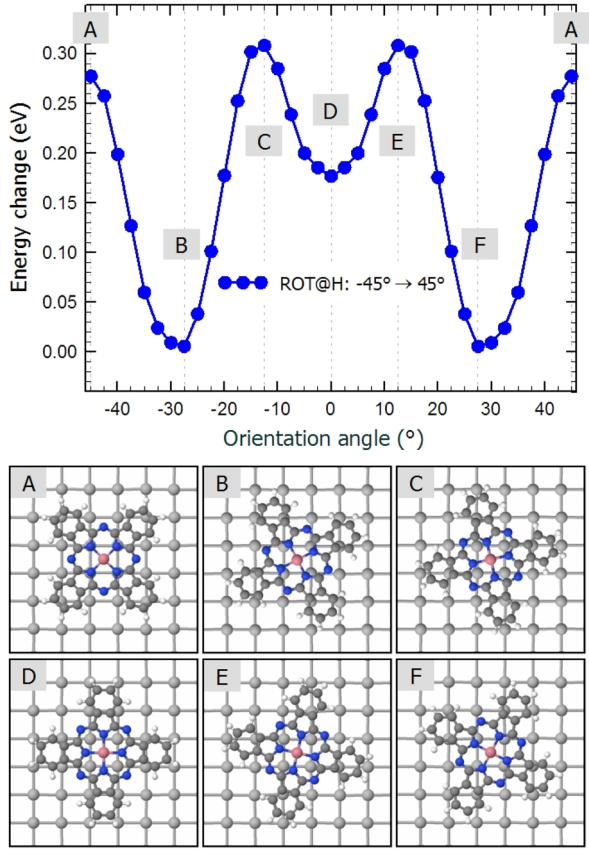

Figure 7. Calculated total energy changes during the rotation of the CoPc molecule at the hollow site (top panel) and top views of the CoPc molecule during the rotation (bottom panel). The letters A−F denote different stages of the CoPc rotation as marked in top panel.

DOI: 10.1021/jacs.5b08001
J. Am. Chem. Soc. 2015, 137, 14920−14929

molecule. The angles are measured with respect to the [110] direction. The angular distance of 90° for rotation of the molecule leads to transformation of a molecule between the same configurations; i.e., +45° and −45° are identical. Figure 7 shows all the barriers experienced by molecule during 90° rotation above the hollow site. From the potential energy barrier in Figure 7 we clearly detect two potential minima of the same depth at ±27.5°, which are associated with the configurations 1 and 2 (see B and F in Figure 7), respectively. Additionally, we see two types of barriers which are associated with the presence of two possible paths leading to the configuration change by the rotation in the hollow site. The first path, with the transition state at 45° (see A in Figure 7) where the four pyrrole nitrogen atoms of the CoPc molecule are located over the Ag surface atoms, is associated with a symmetric barrier of 0.28 eV. The second path leads over the barrier with the metastable state at 0° (see D in Figure 7) and has a barrier height of 0.31 eV. The difference between the metastable and the stable potential minima on this path amounts to 0.18 eV. The energy difference is quite large, and we did not observe experimentally the CoPc molecule in the metastable state.

If the molecule equilibrates at the metastable potential minimum, then its lifetime is clearly not long enough for being imaged in STM. A similar case was previously shown for the metastable walk of a Pt adatom on the Pt(110)−(1 × 2) reconstructed surface.[52,53] The changes in the height of the central Co atom during the rotation in a hollow site are in the range of 0.1 Å. The lowest position of the Co corresponds to the minimum of the total energy. Both energy barriers for the change in configuration by rotation in the hollow site are higher than the experimentally determined energy barrier of 0.19 eV, as presented in scenario 2 (see Table 1).

The next step to reveal the mechanism of motion of the CoPc molecule on the Ag(100) is the translation of CoPc. We start from the most stable configuration derived from the rotation in the hollow site, namely the configuration 1 (see F in Figure 7) and move the molecule in a stepwise manner over the bridge site to the nearest-neighbor hollow site. The change in the total energy of the system is presented in the top panel of Figure 8. The bottom panel of Figure 8 presents two configurations on the translation path of the molecule: at the hollow site (see H in Figure 8) and the transition state at the bridge site (see B in Figure 8). The energy difference between hollow and bridge sites amounts to 0.21 eV, which is also higher than the experimentally determined value of 0.14 eV in scenario 1 as well as 0.15 eV in scenario 2. The CoPc molecule was free to rotate during the translation procedure; however, the changes of the molecular orientation on the translation hollow-to-hollow path are less than 0.2°. The shape of the potential energy landscape is much more complex for this large organic molecule than for single atom diffusion. The height changes of central Co atom of the molecule, presented in inset of Figure 8a, are as much as 0.2 Å, twice as much as during rotation at the hollow site. Again the lowest position of Co atom is correlated to the minimum energy for the system. In the bottom panel of Figure 8 are also presented the side views of the CoPc molecule at the hollow (H) and bridge (B) site. We notice that the molecule is slightly bent out of planarity in the transition state, e.g., at the bridge site (B).

The two attempts to uncover the mechanism of motion of the CoPc molecule on the Ag(100) surface, rotation at the hollow site and translation between the hollow sites, were

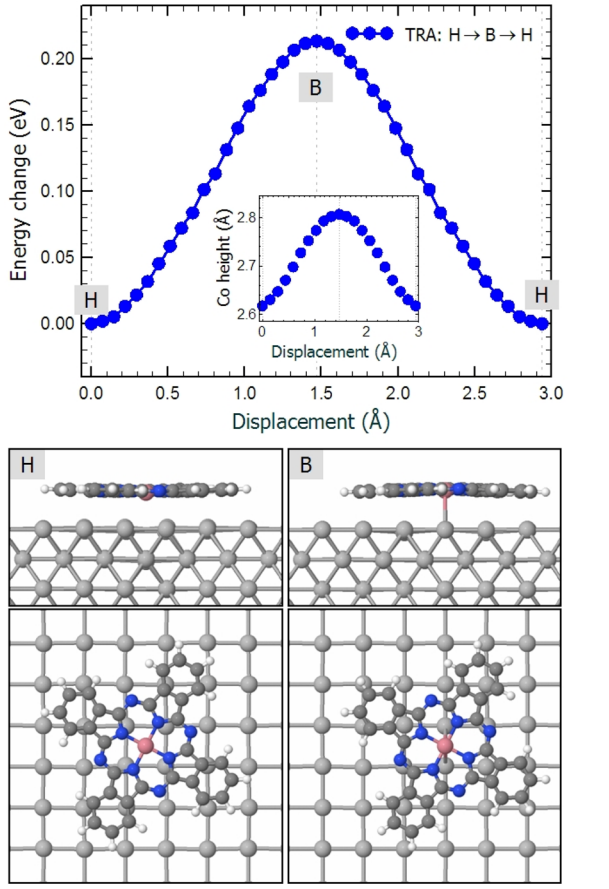

Figure 8. Calculated total energy changes during the translation of the CoPc molecule between the two nearest hollow sites (top panel). The initial molecule orientation was +27.5° with respect to the [110] direction and remained almost unchanged (within 0.2°) on the whole translation hollow-to-hollow path. The inset shows the changes in vertical position of the Co atom during the transition. Bottom panel: side and top views of the CoPc molecule in the hollow (H) and the bridge (B) sites.

assuming that rotation and translation are independent processes. This approach failed to explain the experimental findings; the values do not agree with either scenario 1 or 2 envisioned from experiment. In such a situation we decided to explore the rotation of the CoPc molecule at the bridge site. The changes in total energy are presented in the top panel of Figure 9. The bottom panel shows the molecules during its rotational path at the bridge site.

The potential energy surface for the rotation at the bridge site is much smoother than for the previously described transitions. The observed three barriers are only about 0.1 eV. The height of central Co atom of the molecule changes by only 0.04 Å, and again the minimal distance of Co atom from the surface is observed for the minimum of energy. At this rotational path in the transition state we observe three potential minima: the first at the orientation of +20°, the second at 45°, and third at −20° (see A, C, and E in Figure 9, respectively). Surprisingly, the energy minima are at different orientation angles than at the hollow site, which means that during translation with a fixed angle the molecule is transferred close to a maximum of the potential barrier at the bridge site instead of its minimum. This suggests that translation and rotation are correlated. It is very likely that the molecule gradually changes the orientation angle during the translation. Figure 10 illustrates

DOI: 10.1021/jacs.5b08001
J. Am. Chem. Soc. 2015, 137, 14920−14929

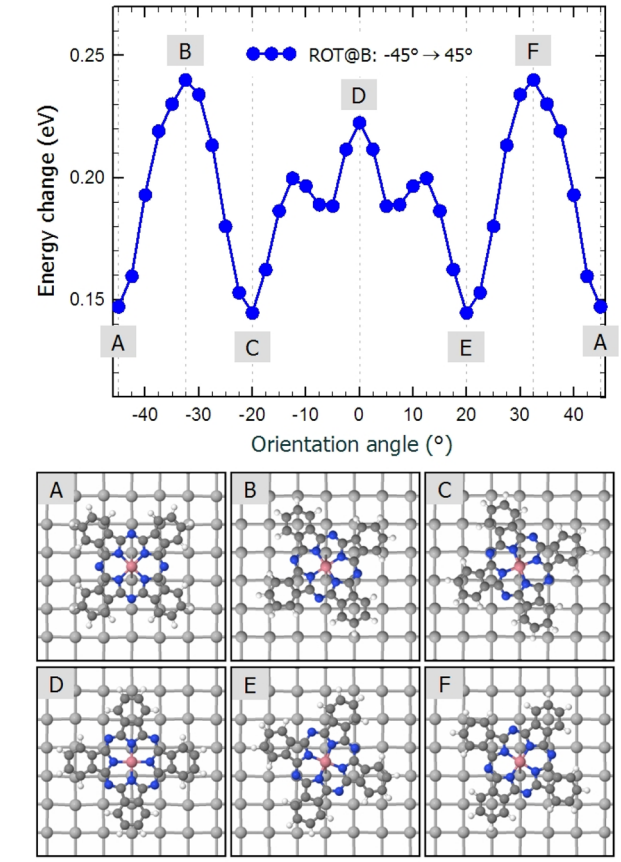

Figure 9. Calculated total energy changes during the rotation of the CoPc molecule at the bridge site (top panel). Top views of the CoPc molecule during this rotation (bottom panel). The letters A–F denote different stages of the rotation as marked in top panel.

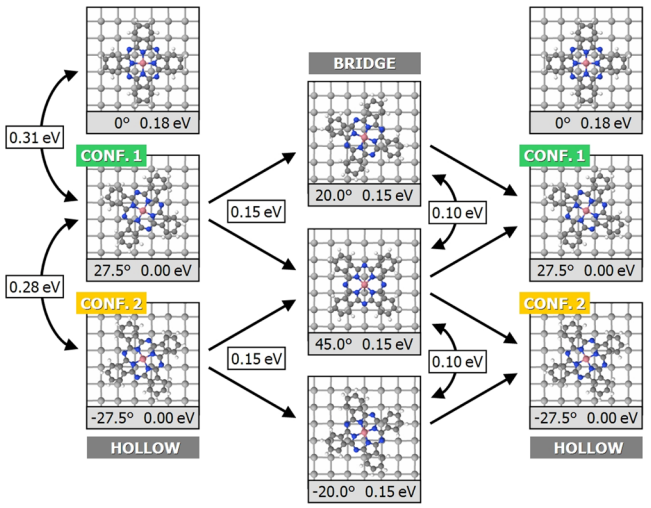

Figure 10. Schematics of energetics from DFT study of possible transitions between stable configurations 1 and 2. CoPc molecule has 4-fold symmetry, and the rotation angles of −20.0° and −27.5° are equivalent to +70.0° and +62.5°, respectively.

the energetics of transitions. If the molecule in configuration 1 moves and rotates counterclockwise, the orientation angle can change from +27.5° at the hollow to +20° at the bridge site. The energy difference between these two configurations amounts to 0.15 eV and nicely agrees with the experimental value for sum of transitions (scenario 3). After crossing the transition state the molecule is likely to come back to the orientation angle of +27.5° since in this way it needs to move only over the angular distance of 7.5°. Such event will be observed experimentally as translation of a molecule between the same configurations. If the molecule in configuration 1 starts to move over the surface and rotates clockwise, then it has to reach the transition state at 45° (see A in Figure 9). The energy difference for such transition is also 0.15 eV, again perfectly matching the experimental values (scenario 3). However, for such a channel continuation from the transition state to the stable adsorption site can have two equally probable outcomes. The molecule can continue to rotate to the stable +62.5° (configuration 2), which is the same as −27.5° due to 4-fold symmetry molecule and the surface. The molecule can also start to rotate counterclockwise at the transition state and land in stable configuration 1 (+27.5°). The experimentally observed outcome of such event will be rotation or translation, respectively. The mirror-like events will be observed for a molecule which starts to move from configuration 2. The transition states for such molecule will be at orientation angles of −20° and 45°.

Two transitions paths available for each configuration explain the higher occurrence of translation than rotation, since translation can be realized by two channels: over ±20° and 45° transition states, while rotation can be realized only over 45° transition state. Both paths are associated with the same activation energy of 0.15 eV, which agree with the experimental scenario 3.

The observed (not frequent) rotations at the hollow site might be due to rotation at the hollow site but are (more likely) the result of a coming back of the molecule to the original adsorption site after having started a translational–rotational motion to the bridge site (intracell motion).

On the basis of the agreement of the experimental (scenario 3) to the theoretical findings, we conclude that translation and rotation of the CoPc molecule on the Ag(100) surface are interconnected. The motion over the surface is realized by a combined translational–rotational motion of the molecule. The standard frequency factor in the range of 10^{13} s^{-1} for the sum of all events also supports such an explanation of the process.

This model also explains almost 4 times higher rates of translation compared to rotation observed in experiment. Assuming an equal probability for both (20° and 45°) channels, our theoretical model leads to a ratio of 3:1 for translation versus rotation because of the larger number of paths for translation. However, considering the angular distance of both transition states from the ground state, one can expect that the 20° transition state (angular distance from the hollow only 7.5°) is more probable than the 45° transition state (angular distance from the hollow 17.5°). That explains why we observe a higher ratio of translations to rotation then expected 3:1 ratio.

V. CONCLUSIONS

We investigated the adsorption and diffusivity of the CoPc molecule on Ag(100). The CoPc molecule adsorbs in two equally probable configurations, which are mirror-like images with respect to the [110] direction of the surface. In the stable configuration the molecules are with the central Co atom above the hollow site of the surface and are rotated by around ±27.5° from the [110] direction.

We found that the motion on Ag(100) is 2D, and the deformation of the molecule, visible in the STM images, does

DOI: 10.1021/jacs.5b08001
J. Am. Chem. Soc. 2015, 137, 14920–14929

not influence the dimensionality of motion. The motion on the time scale of minutes starts at around 40 K and requires the activation energy of 0.16 eV. The prefactor of diffusivity is in the range of 10^{-1} cm^2/s, which is most likely associated with complex character of motion.

The CoPc molecules translate and rotate during their motion over the surface. We explore a possibility of a correlation of these two transitions. Our combined STM and DFT investigations suggest that translation and rotation are not independent of each other. The molecule gradually rotates during translation to the nearest-neighbor adsorption site. Displacement of the center-of-mass of the molecule can happen through two channels: over ±20° and 45° transition state. When it moves over ±20° transition state, then after crossing the transition state it rotates back to the stable ±27.5° hollow site. When it moves through 45° transition state, then it can come back to the +27.5° stable orientation or continue to rotate to the −27.5° also stable configuration. The higher jump rates observed for translations in the experiment can be understood by moving to the nearest-neighbor adsorption site through two equally energetically demanding channels. The configuration change can be achieved only by one channel.

Translation is associated with the displacement of the center-of-mass of the molecule and affects the transport of material. Rotation provides the possibility of growth of a uniform molecular film. We show that both transitions are mutually interconnected. Beyond the specific case investigated here, we line out that several degrees of freedom of the molecule (here rotation around the surface normal) have to be considered to understand the motion of larger molecules.

■ ASSOCIATED CONTENT

Supporting Information

The Supporting Information is available free of charge on the ACS Publications website at DOI: 10.1021/jacs.5b08001.

Movie of CoPc thermal diffusion (AVI)

STM image of adsoption of CoPc after annealing (Figure S1), map of adsorption places visited (Figure S2) (PDF)

■ AUTHOR INFORMATION

Corresponding Author

*E-mail: antczak@ifd.uni.wroc.pl (G.A.).

Notes

The authors declare no competing financial interest.

■ ACKNOWLEDGMENTS

The project was supported by the Humboldt Stiftung as part of G.A. Humboldt Fellowship stay at the Leibniz University Hanover. W.K. and G.A. thank the project number 1010/S/IFD/15 for support. A.S. thanks the project number 2457/M/IFD/14 for support. Numerical calculations were performed at the Interdisciplinary Center for Mathematical and Computational Modelling of the University of Warsaw within the Grant No. G44-10. K.M. acknowledges financial support from the Deutsche Forschungsgemeinschaft.

■ REFERENCES

(1) Downes, J. E.; McGuinness, C.; Glans, P. A.; Learmonth, T.; Fu, D.; Sheridan, P.; Smith, K. E. *Chem. Phys. Lett.* **2004**, *390*, 203.

(2) Hu, Z.; Li, B.; Zhao, A.; Yang, J.; Hou, J. G. *J. Phys. Chem. C* **2008**, *112*, 13650.

(3) Neghabi, M.; Zadsar, M.; Ghorashi, S. M. B. *Mater. Sci. Semicond. Process.* **2014**, *17*, 13.

(4) Paoletti, A. M.; Pennesi, G.; Rossi, G.; Generosi, A.; Paci, B.; Albertini, V. R. *Sensors* **2009**, *9*, 5277.

(5) Warner, M.; Din, S.; Tupitsyn, I. S.; Morley, G. W.; Stoneham, A. M.; Gardener, J. A.; Wu, Z.; Fisher, A. J.; Heutz, S.; Kay, C. W. M.; Aeppli, G. *Nature* **2013**, *503*, 504.

(6) Zaho, A.; Li, Q.; Che, L.; Xiang, A.; Wang, W.; Pan, S.; Wang, B.; Xiao, X.; Yang, J.; Hou, J. G.; Zhu, Q. *Science* **2005**, *309*, 1542.

(7) Chiappe, G.; Louis, E. *Phys. Rev. Lett.* **2006**, *97*, 076806.

(8) Zhao, A.; Hu, Z.; Wang, B.; Xiao, X. D.; Yang, J. L.; Hou, J. G. *J. Chem. Phys.* **2008**, *128*, 234705.

(9) Antczak, G.; Ehrlich, G. *Surface Diffusion: Metal, Metals atoms and Clusters*; Cambridge University Press: Cambridge, 2010.

(10) Jurczyszyn, L.; Antczak, G. *Appl. Surf. Sci.* **2014**, *299*, 146.

(11) Fijak, R.; Jurczyszyn, L.; Antczak, G. *Surf. Sci.* **2013**, *608*, 115.

(12) Morgenstern, K.; Braun, K.-F.; Rieder, K.-H. *Phys. Rev. Lett.* **2004**, *93*, 056102.

(13) Heidorn, S.-Ch; Bertram, C.; Cabrera-Sanfelix, P.; Morgenstern, K. *ACS Nano* **2015**, *9*, 3572.

(14) Zaum, C.; Meyer auf de Heide, H.; McDonough, S.; Schneider, W.; Morgenstern, K. *Phys. Rev. Lett.* **2015**, *114*, 146104.

(15) Dobbs, K. D.; Doren, D. J. *J. Chem. Phys.* **1993**, *99*, 10041.

(16) Skaug, M. J.; Mabry, J. N.; Schwartz, D. K. *J. Am. Chem. Soc.* **2014**, *136*, 1327.

(17) Luedtke, W. D.; Landman, U. *Phys. Rev. Lett.* **1999**, *82*, 3835.

(18) Mugarza, A.; Robles, R.; Krull, C.; Korytár, R.; Lorente, N.; Gambardella, P. *Phys. Rev. B: Condens. Matter Mater. Phys.* **2012**, *85*, 155437.

(19) Chang, S. H.; Kuck, S.; Brede, J.; Lichtenstein, L.; Hoffmann, G.; Wisendanger, R. *Phys. Rev. B: Condens. Matter Mater. Phys.* **2008**, *78*, 233409.

(20) Chiang, C.-I.; Xu, C.; Han, Z.; Ho, W. *Science* **2014**, *344*, 885.

(21) Guo, Q.; Qin, Z.; Zang, K.; Liu, C.; Yu, Y.; Cao, G. *Langmuir* **2010**, *26*, 11804.

(22) Lu, X.; Hipps, W.; Wang, X. D.; Mazur, U. *J. Am. Chem. Soc.* **1996**, *118*, 7197.

(23) Weckesser, J.; Barth, J. V.; Kern, K. *J. Chem. Phys.* **1999**, *110*, 5351.

(24) Weckesser, J.; Barth, J. V.; Kern, K. *Phys. Rev. B: Condens. Matter Mater. Phys.* **2001**, *64*, 161403.

(25) Loske, F.; Lübbe, J.; Schütte, J.; Reichling, M.; Kühnle, A. *Phys. Rev. B: Condens. Matter Mater. Phys.* **2010**, *82*, 155428.

(26) Schunack, M.; Linderoth, T. R.; Rosei, F.; Lægsgaard; Stensgaard, I.; Besenbacher, F. *Phys. Rev. Lett.* **2002**, *88*, 156102.

(27) Kwon, K. Y.; Wong, K. L.; Pawin, G.; Bartels, L.; Stolbov, S.; Rahman, T. S. *Phys. Rev. Lett.* **2005**, *95*, 166101.

(28) Wong, K. L.; Pawin, G.; Kwon, K. Y.; Lin, X.; Jiao, T.; Solanki, U.; Fawcett, R. H. J.; Bartels, L.; Stolbov, S.; Rahman, T. S. *Science* **2007**, *315*, 1391.

(29) Raut, J. S.; Fichthorn, K. *J. Vac. Sci. Technol. A* **1997**, *15*, 1542.

(30) Yokoyama, T.; Takahashi, T.; Shinozaki, K. *Phys. Rev. B: Condens. Matter Mater. Phys.* **2010**, *82*, 155414.

(31) Eichberger, M.; Marschall, M.; Reichert, J.; Weber-Bargioni, A.; Auwärter, W.; Wang, R. L. C.; Kreuzer, H. J.; Pennec, Y.; Schiffrin, A.; Barth, J. V. *Nano Lett.* **2008**, *8*, 4608.

(32) Buchner, F.; Xiao, J.; Zillner, J.; Chen, M.; Röckert, M.; Ditze, S.; Stark, M.; Steinrück, H. P.; Gottfried, J. M.; Marbach, H. *J. Phys. Chem. C* **2011**, *115*, 24172.

(33) Ikonomov, J.; Bach, P.; Markel, R.; Sokolowski, M. *Phys. Rev. B: Condens. Matter Mater. Phys.* **2010**, *81*, 161412.

(34) Hahne, S.; Ikonomov, J.; Sokolowski, M.; Maass, P. *Phys. Rev. B: Condens. Matter Mater. Phys.* **2013**, *87*, 085409.

(35) Hahne, S.; Maass, P. *J. Phys. Chem. A* **2014**, *118*, 2237.

(36) Mehlhorn, M.; Gawronski, H.; Nedelmann, L.; Grujic, A.; Morgenstern, K. *Rev. Sci. Instrum.* **2007**, *78*, 033905.

(37) Horcas, I.; Fernández, R.; Gómez-Rodríguez, J. M.; Colchero, J.; Gómez-Herrero, J.; Baro, A. M. *Rev. Sci. Instrum.* **2007**, *78*, 013705.

DOI: 10.1021/jacs.5b08001
J. Am. Chem. Soc. 2015, 137, 14920−14929

(38) Kresse, G.; Furthmüller, J. *Phys. Rev. B: Condens. Matter Mater. Phys.* **1996**, *54*, 11169.
(39) Kresse, G.; Joubert, D. *Phys. Rev. B: Condens. Matter Mater. Phys.* **1999**, *59*, 1758.
(40) Perdew, J. P.; Burke, K.; Ernzerhof, M. *Phys. Rev. Lett.* **1996**, *77*, 3865.
(41) Grimme, S. *J. Comput. Chem.* **2006**, *27*, 1787.
(42) Carrasco, J.; Liu, W.; Michaelides, A.; Tkatchenko, A. *J. Chem. Phys.* **2014**, *140*, 084704.
(43) Li, S.; Hao, J.; Li, F.; Niu, Z.; Hu, Z.; Zhang, L. *J. Phys. Chem. C* **2014**, *118*, 27843.
(44) Yildirim, H.; Rahman, T. S. *Phys. Rev. B: Condens. Matter Mater. Phys.* **2009**, *80*, 235413.
(45) Langewisch, G.; Kamiński, W.; Braun, D.-A.; Möller, R.; Fuchs, H.; Schirmeisen, A.; Pérez, R. *Small* **2012**, *8*, 602.
(46) Antczak, G.; Kamiński, W.; Morgenstern, K. *J. Phys. Chem. C* **2015**, *119*, 1442.
(47) Davey, W. P. *Phys. Rev.* **1925**, *25*, 753.
(48) Bader, R. F. W.; Henneker, W. H.; Cade, P. E. *J. Chem. Phys.* **1967**, *46*, 3341.
(49) Szybowicz, M.; Bała, W.; Dümencke, S.; Fabisiak, K.; Paprocki, K.; Drozdowski, M. *Thin Solid Films* **2011**, *520*, 623.
(50) Cuadrado, R.; Cerda, J. I.; Wang, Y.; Xin, G.; Berndt, R.; Tang, H. *J. Chem. Phys.* **2010**, *133*, 154701.
(51) Antczak, G.; Kamiński, W.; Sabik, A.; Morgenstern, K. Unpublished.
(52) Linderoth, T. R.; Horch, S.; Lægsgaard, E.; Stensgaard, I.; Besenbacher, F. *Phys. Rev. Lett.* **1997**, *78*, 4978.
(53) Lorensen, H. T.; Nørskov, J. K.; Jacobsen, K. W. *Phys. Rev. B: Condens. Matter Mater. Phys.* **1999**, *60*, R514.

DOI: 10.1021/jacs.5b08001
J. Am. Chem. Soc. 2015, 137, 14920−14929